

**Characterization of Macromolecular Solutions by Combined
Static and Dynamic Light Scattering Technique¹**

S.V. Kazakov^{2,3}, I.Yu. Galaev² and Bo Mattiasson^{2,4}

¹ Paper presented at the Fourteenth Symposium on Thermophysical Properties, June 25-30, 2000, Boulder, Colorado, U.S.A.

² Department of Biotechnology, Center for Chemistry and Chemical Engineering, Lund University, P.O. Box 124, S-221 00, Lund, Sweden

³ Guest scientist from Faculty of Physics, Lomonosov Moscow State University, 119899 Moscow, Russia

⁴ To whom correspondence should be addressed.

Present address: Department of Biotechnology, Chemical Center, University of Lund, POB 124, Lund SE 22100, Sweden, Tel: +46 46 2228264, Fax: +46 46 2224713, E-mail: <Bo.Mattiasson@biotek.lu.se>.

ABSTRACT

The combination of quasielastic LS with integrated scattered intensity measurements in the same sample has been applied to study polymer and polymer-protein aqueous solutions. The molecular weight, the radius of gyration, and the second virial coefficient for thermosensitive polymer [poly(N-isopropylacrylamid)] solution before and after precipitation transition have been obtained using Zimm plot calculations carried out. The precipitation curve (intensity vs temperature dependence) for polymer solutions has been experimentally obtained using the light scattering setup. For the first time the static and dynamic light scattering properties of aqueous solutions of antibody-poly(methacrylic acid) and antibody-poly(acrylic acid) conjugates and solutions of their components [antibody, poly(methacrylic acid), and poly(acrylic acid)] at different pH values have been measured. In both cases the parallel comparison of the characteristic size variations allowed us to represent novel structural features of scattered particles (macromolecules, associates, aggregates, conjugates, colloidal particles) in studied systems.

KEY WORDS: aggregation, association, conjugate, co-operative interactions, light scattering, polymer, precipitation, protein.

1. INTRODUCTION

Light scattering (LS) is a highly informative method and the combination of quasielastic LS and integrated scattered intensity measurements in the same experimental setup increases the gain of virtual information of the systems studied [1]. Recently, photon correlation spectroscopy (PCS) has become a popular technique for studying structural transformations in systems, containing proteins, enzymes, polymers, and other macromolecular components [2,3].

Table 1 presents parameters which could be calculated out of the data of static and dynamic LS. The first line gives the formula for concentration and angular dependencies of static and dynamic Zimm plots. The second line presents the experimental parameters along with the limitations of using these expressions imposed on c and Θ . The remaining parameters can be compared as equivalent sphere radii that are represented in the next line of the Table 1. From static LS one gets two effective sizes: radius of gyration, R_g , and thermodynamic radius, R_T , from dynamic LS – hydrodynamic radius, R_h . The magnitudes of these radii can deviate from each other [4]. These differences result from the fact that they are physically differently defined. R_g is solely geometrically defined, but there are two types of interaction between particles in solution of finite concentration: hydrodynamic and thermodynamic.

The hydrodynamic interaction is characterized by R_h indicated how deeply a particle is drained by the solvent: a deep draining causes a reduction in R_h , on the other hand, if shallow draining is only possible, R_h can become much larger than R_g . The thermodynamic interactions (repulsion or attraction) are characterized by the thermodynamically effective equivalent sphere radius R_T , which is defined by the domains of interpenetration of two macromolecules or in other words by the excluded

volume. Generalized ratios of these differently defined radii can be derived. The ratio $\rho = R_g/R_h$ compares the range of hydrodynamic interaction with geometrical dimensions of the molecule and can be theoretically calculated for the selected structures. For example, for a homogeneous sphere ρ is less than unity, for microgels it can be less than 0.5, for random coil it changes from 1.5 to 2 depending on polydispersity, solvent, and conditions, for rigid rod it is greater than 2. The ratio $V_T = R_T/R_h$ compares the range of thermodynamic interactions with that of hydrodynamic interactions. Experiments mostly demonstrate that the ratio is close to unity, it means that the thermodynamic and hydrodynamic interactions act over very similar distances.

Thus, it follows from the analysis of Table 1 that a complete picture of structural features of scattered particles in solution can be obtained by parallel correlation of characteristic sizes between each other which are the result of static and dynamic LS measurements in the same sample and at the identical experimental conditions. We demonstrate these opportunities on the example of application LS technique to the study of the precipitation of one of the well-known thermosensitive polymer, poly(N-isopropylacrylamid) (PNIPAM), determining the temperature of phase transition in aqueous solution and measuring molecular weight, radius of gyration, and the second virial coefficient before and after the transition.

Moreover, in this paper we focus on the molecular and structural parameters of poly(methacrylic acid) (PMAA), poly(methacrylic acid) (PAA), antibodies and their conjugate with PMAA and PAA in aqueous solutions determined by static and dynamic LS. Particular attention is given to the elucidation of the interdependence of the components affecting the association and aggregation of the conjugates.

The study of the protein-polymer conjugates in which the role of protein is played

by antibody (Ab) is of special interest. Antibody is attractive as the protein model. In spite of a great variety of antibodies their molecules are structurally similar and characterized by virtually the same isoelectric point. To us, the Ab-polymer systems are of particular interest for several reasons: (i) A study on the features of Ab-polymer conjugates and variation of their structure with pH is a prerequisite to understanding the higher-order systems (e.g., complexes of two conjugates)[5,6]. (ii) An investigation and recognition of the role of the constituents of the conjugates is crucial for understanding their aggregation and precipitation. In turn, the control of association and aggregation processes in the multicomponent systems is essential for the development of bioseparation method and specific assays. (iii) Protein-polymer complexes have been studied with many experimental methods [7,8].

There is still a lot of theoretical and experimental problems hindering the obtaining of reliable data from PCS measurements. However, in the particular case of pronounced aggregation the significant variations in macromolecular size of the associated species provide a straightforward interpretation of the PCS results. To the best of our knowledge aqueous solutions of antibody and in particular the behavior of antibodies and their conjugates with polyelectrolytes in response to pH have not been studied using LS technique.

2. MEASUREMENTS

2.1. Specimens

Milli-Q water with $R \approx 18 \text{ M}\Omega\text{-cm}$ and 10 mM phosphate buffer, containing 0.1 M NaCl, were used in all experiments.

Monoclonal antibodies from 6C5 clone against inactivated rabbit muscle glyceraldehyde-3-phosphate dehydrogenase were raised in mice and characterized by

their binding to native and inactivated forms of the enzyme [9]. Ab concentration was determined by UV absorbance measuring at 280 nm (E_{280} for 0.1 % was equal 1.5). Stock Ab solution with initial concentration of Ab 1.48 mg/ml was diluted to 0.74 mg/ml before LS measurements. Isoelectric point of Ab (pI 5.95) was determined previously [11]. Synthesis of PMAA and PAA with a degree of polymerization of 1830 and 3200 respectively is described elsewhere [4,5].

Stock solution of PMAA was prepared with the concentration of 38.3 mg/ml, diluted to 4.8 mg/ml, and then filtered using 0.2 μm Sartorius Minisart filter into the $\text{\O}10$ mm sample cell. Initial pH of this sample was 5.0. Stock solution of PAA was prepared with the concentration of 2.9 mg/ml, diluted to 0.091 mg/ml, and then filtered using 0.2 μm Sartorius Minisart filter into the $\text{\O}10$ mm sample cell. Initial pH of this sample was 5.8.

Conjugates of PMAA and PAA with the antibodies (Ab-PMAA and Ab-PAA) were synthesized by covalent binding using a procedure including water-soluble carbodiimide [4,5]. The stock Ab-PMAA solution with concentration 1 mg/ml was diluted four times and then filtered using 0.2 μm Sartorius Minisart filter into the quartz $\text{\O}10$ mm sample cells. The Ab-PAA solution with concentration 0.85 mg/ml was filtered using 0.2 μm Sartorius Minisart filter into the quartz $\text{\O}10$ mm sample cells. pH of all solutions was adjusted by adding correspondent amount of 0.1 M HCl solution or 0.2 M NaOH solution.

PNIPAM was synthesized by radical polymerization in aqueous solution at room temperature using redox pair ammonium persulphate–tetraethylene methylenediamine (TEMED) as initiator and purified by three sequential reprecipitations at 40°C. For Zimm plot measurements (angular and concentration dependence of the excess Rayleigh

ratio, see Table 1) four aqueous solutions of PNIPAM with different concentration (0.38, 0.29, 0.19, and 0.096 mg/ml) were prepared and filtered using 0.2 μm Sartorius Minisart filter into the quartz $\varnothing 10$ mm sample cells. Precipitation curve was obtained for the solution with concentration 0.019 mg/ml.

2.2. Light Scattering

LS measurements were done with a Malvern 4700c System. An argon ion laser (Uniphase 2213-75 SL) operating at a 488 nm wavelength and 30 mW output power was used as a light source. The scattering angle was varied from 30° to 150° in 13 steps. The spectrometer was calibrated with distilled water and toluene to make sure that the scattering intensity from water and toluene had no angular dependence in the used angular range. All measurements were performed at $(25.0 \pm 0.1)^\circ\text{C}$.

In static LS we used an angle scan with axes of inverse intensity vs q^2 , to calculate radius of gyration R_g :

$$I_{\Theta}^{-1}(q) \cong I_0^{-1} \left(1 + \frac{1}{3} R_g^2 q^2 \right), \quad (1)$$

In this equation I_{Θ}^{-1} is an inverse scattering intensity at scattering angle Θ . The limit $qR_g < 2$ was fulfilled within the range of scattering angles for all systems studied.

The intensity-intensity time autocorrelation functions of the scattered intensity in the self-beating mode can be related to the normalized first-order electric field time correlation function $g^{(1)}(t, q)$ as

$$G^{(2)}(t) = \langle I(0)I(t) \rangle = B[1 + \beta |g^{(1)}(t, q)|^2], \quad (2)$$

where β is a parameter depending on the coherence of the detection, t is the delay time, and B a measured baseline. Logarithmic correlation function can be expanded in a power series in terms of the delay time (cumulant analysis)

$$\ln g^{(1)}(t) = -\Gamma_1 t + (\Gamma_2 / 2!)t^2 - (\Gamma_3 / 3!)t^3 + \dots, \quad (3)$$

where Γ_1 , Γ_2 , etc are the first, second, etc cumulants. The first cumulant can be calculated by equilibrium statistical thermodynamics and at low q related to the apparent diffusion coefficient D : $\Gamma_1 = Dq^2$. “Z-average particle size” can be found using well-known Stokes-Einstein relationship, which is a definition for a hydrodynamically effective sphere diameter $\langle d_h \rangle$ (see Table 1). If the sample is polydisperse, the value $2\Gamma_2/\Gamma_1^2 = \text{PI}$, the polydispersity index (the width of the distribution), which is the dimensionless measure of the broadness of the distribution.

Dynamic measurements were performed as follows. The scattering angle was kept constant at 90° . The quality of measurement was checked over the signal-to-noise ratio and the range of the correlation function. The intensity autocorrelation function was collected in 128 channels and in a so-called far point, a special group of correlator channels pushed out in time by a special extension of the memory. The difference between the measured and the calculated baselines is taken into account. It was found out that the field-field correlation function is single-exponential for all samples studied. The particle size distribution and average particle size were obtained from the correlation function by fitting the data with cumulant analysis, using the PCS software program (version 1.35) supplied by Malvern Instruments Ltd.

3. RESULTS AND DISCUSSION

3.1. Phase transition of PNIPAM

It is known that scattered intensity is proportional to the spatial fluctuations of concentrations $I \sim \langle \Delta c^2 \rangle$ and one can expect that this value could be more sensitive when approaching the cloud point of the polymer. We have used this fact for the determination of the temperature of phase transition in aqueous solution of

thermosensitive polymer PNIPAM (Fig.1). A conformational random coil-globule transition for PNIPAM before phase transition is well documented [12] in extremely diluted solutions. We have shown this effect for rather concentrated solutions.

Static LS measurements (angular and concentration dependencies) have been carried out at 23 and 37 °C, i.e. before and after the transition: points are indicated on the precipitation curve (Fig.1). The typical Zimm plot calculated by Malvern Instruments Ltd software is presented in Fig.2. Table 2 gives the extracted parameters: M_w , R_g , and A_2 . These data indicate that aggregates with 60-fold greater molecular weight but two times less size are formed after transition. The aggregates exist in solution as a stable suspension. Significant decrease in the second virial coefficient corresponds to the solution of Θ -conditions. The values of R_T before and after the phase transition, i.e. as for random coils and for aggregates of globules, indicate strong polymer-polymer interaction expressed in significant overlapping areas.

3.2. Conjugates and their free components characterization

3.2.1. Polymers

The parameters of PMAA obtained by combined static and dynamic LS at different values of pH are presented in Figs.3, 4 (PMAA). As expected, no aggregation or precipitation occurred over the whole studied range of pH. However polymer chains co-operatively expanded forming more homogeneous medium with increasing pH. Z-average radius of gyration R_g has been increased sharply at $\text{pH} > 5$ (Fig.3a, PMAA). Parameter $\langle d_h \rangle$ appeared to be less sensitive to the changes of scattering particles shape in this case (Fig.4a, PMAA). A set of data on R_g and $\langle d_h \rangle$ obtained allows to conclude that PMAA chains expansion (increasing of R_g) is accompanied with the retention of the domain sizes $\langle d_h \rangle$ of effective polymer-solvent

interactions. Herein, numeric values of the ratio $2\langle R_g \rangle / \langle d_h \rangle$ varied in the range 1.75-2.5 with which limit values are typical for the molecules of polymer with the structure of random coils in Θ -conditions and good solvent, respectively. The decrease in LS intensity (Fig.3b, PMAA) which was proportional to the concentration fluctuations indicated more homogeneous state of co-operatively expanded polymer chains. On the other side, it is obvious that a more compact form of polymer has to have fewer deviations in molecular size, and vice versa. This fact was reflected in the increase in PI at $\text{pH} > 5$ (Fig.4b, PMAA).

The properties of PAA are expected to differ sharply from those of PMAA although the only difference in the chemical structures of these polyacids consists in the methyl groups in the α position of the PMAA molecules [6,10]. The data on static and dynamic LS measurements of PAA solutions presented in Figs.3, 4 (PAA) demonstrate no conformational transition of PAA molecules in the whole interval of pH values studied (2.5 – 9), confirming that the hydrophobic interactions of methyl groups in PMAA are responsible for the stability of the local compact structures in this polyacid molecules in acidic medium and for their co-operative expansion in the neutral medium.

3.2.2. Antibody

The protein solubility decreases around isoelectric point. In our experiments the precipitation of Ab molecules was observed after the addition of 0.5 M HCl when pH changed from 6.8 to 5.9, in the region closed to pI of the antibodies (pI 5.95). The pH-dependencies of radius of gyration (a), light scattering intensity (b), hydrodynamic diameter (c), and polydispersity index (d) of antibodies are presented in Figs.3, 4. The precipitation at pH about 6.0 (marked by dotted lines in the figure) is accompanied by significant variations of overall measured characteristics, indicating the pronounced

association of Ab molecules. The further evidence of the association of free antibodies could be derived from the comparison of their size with the size of the antibodies-poly(methacrylic) acid conjugate.

3.2.3. *Polymer-protein conjugates*

The data of static and dynamic LS for the Ab-PMAA conjugates indicated the shift of the precipitation transition for Ab-PMAA conjugate to more acidic medium (pH~4.8) as compared to the solution of free Ab (pH ~ 6) (Figs.3, 4, Ab-PMAA).

The comparison of LS data for Ab solution with the data for the solution of Ab-PMAA conjugates highlights the effect of PMAA on the ability of Abs to associate. The covalent attachment of a charged polymer to Ab molecule prevents the latter from approaching each other and associating.

The next experimental fact obtained for the solution of Ab-PMAA conjugate is a decrease in R_g (Fig.3a, Ab-PMAA) and $\langle d_h \rangle$ (Fig.4a, Ab-PMAA), as well as an increase in I_{90} (Fig.3b, Ab-PMAA) and PI (Fig.4b, Ab-PMAA) in the range of pH 5-6 which precedes the precipitation of Ab-PMAA conjugates at pH~4.8. These changes of LS parameters are directly connected with the co-operative shrinkage of PMAA polymer chains. Thus, there are strong grounds to believe that the compact conformation of PMAA in acidic media is mainly responsible for the observed precipitation of Ab-PMAA conjugates.

Some assumptions about the structure of the conjugates could be done from the comparison of the LS parameters of Ab-PMAA conjugates and free PMAA.

In neutral medium before precipitation R_g of conjugates (Fig.3a, Ab-PMAA) is less than the corresponding size of co-operatively expanded coils of PMAA (Fig.3a, PMAA). This fact testifies that strong interaction between polymer chains and protein

favors the compact arrangement of polymer chains around the protein globule. The geometrical size (R_g) of the conjugate slightly decreased in the pH interval 5-6, whereas the hydrodynamic size ($\langle d_h \rangle$) of the conjugate decreased more essentially reflecting cooperative shrinkage of the polymer coil around the protein globule. At the same time, $\langle d_h \rangle$ of the conjugate significantly exceeded $\langle d_h \rangle$ of free polymer. It strongly indicates that the protein globule gains an interaction of the conjugate with the molecules of the solvent. A hydrated shell is formed around the conjugate. The shell is penetrated by the polymer chain and the thickness of the shell vary depending on the conformational state of the polymer.

To confirm this proposed structure of the polymer-protein conjugate, PAA with significantly higher degree of polymerization than PMAA was selected for covalent attachment to Ab and formation Ab-PAA conjugate. Contrary to PMAA, PAA has no α -methyl groups in polymer chains and as a result no conformational transformations were observed in the pH range studied (Fig.3, 4, PAA). Static and dynamic LS parameters of the Ab-PAA conjugate solution at different pH values are presented in Figs.3 and 4 (Ab-PAA). There was no precipitation in the whole range of pH (2.5 – 8.0), but the behavior of all measured parameters was quite different in neutral (pH 4.8-8.0) and acidic (pH < 4.8) media.

In neutral medium both static and dynamic characteristics almost did not vary with pH. Again, the values of both R_g and $\langle d_h \rangle$ for Ab-PAA conjugate were less than corresponding values for free Ab indicating an ability of the polymer to prevent the association of protein molecules.

The increase of the average radius of gyration (Fig.3a, Ab-PAA) and the average hydrodynamic diameter (Fig.4a, Ab-PAA) of scattering particles was found in acidic

medium of Ab-PAA conjugate solution. This fact as well as a sharp increase in the scattering intensity (Fig.3b, Ab-PAA) along with initial decrease in the polydispersity index on the first stage (Fig.4b, Ab-PAA) unambiguously testifies that the process of aggregation starts at $\text{pH} < 4.8$. An increase in the opalescence of the solution has been observed at $\text{pH} < 4.8$ but solution remained completely homogeneous indicating no precipitation. Under further decrease in pH the elevation of $\langle d_h \rangle$, I_{90} , and the drop of PI slowed down in the range of pH 3-4. The calculations of R_g using Eq.(1) were impossible in this range due to the strong asymmetry of angular dependence of scattering intensity. This is indicated by dotted arrow in Fig.3a (Ab-PAA). At $\text{pH} < 3$ the sharp increase in $\langle d_h \rangle$ and PI took place, probably because colloid particles of Ab-PAA conjugates start binding to each other. As a result the decrease in scattering intensity at $\text{pH} < 3$ (Fig.3b, Ab-PAA) could be explained by progressive influence of the multiple scattering. However in this pH range, even under colloidal particle formation, the solution remains stable, homogeneous, and transparent, i.e. there is no precipitation. The particles are stabilized by electrostatic repulsion caused by still sufficiently high charge density of PAA coil even in acidic medium ($3 < \text{pH} < 4.8$) preventing the system from precipitation and/or a hydrated shell formed by water molecules bound to COOH-groups of PAA via hydrogen bonds.

The average values of R_g (Fig.3a, PAA) and $\langle d_h \rangle$ (Fig.4a, PAA) for the free PAA appear to be higher than the sizes of Ab-PAA conjugates (Figs.3a and 4a, PAA) over the whole range of pH (4.8 –8.0). It could mean that after attachment of the polymer to the protein the latter surrounds the surface of Ab in a compact manner. Essential excess of hydrodynamic radius over radius of gyration indicates strong interactions of conjugate with solvent molecules. At the same time the characteristic

dimensions of different conjugates appear to be close to each other despite the difference in polymer chain lengths of PMAA and PAA attached.

4. CONCLUSIONS

The results presented clearly demonstrate that the combination of static and dynamic LS gives real perspectives in analysis of the structural and molecular characteristics of thermosensitive polymers, proteins, and polymer-protein complexes in solution, and their aggregation and precipitation near phase transitions. The comparison of physically different characteristic molecular dimensions (radius of gyration, thermodynamic radius, and hydrodynamic radius) along with another static and dynamic parameters (scattering intensity, PI) is a powerful tool for developing the structure models of the macromolecular systems.

In particular, the results of our investigation of LS parameters for PMAA, PAA, antibody, and for conjugates formed on the basis of the polymer confirm: (a) that the conformational compactness of the polymer plays crucial role in the process of precipitation, (b) that attached polymer prevents the association of polymer-protein conjugates, (c) that after attachment of the polymer to Ab the former surrounds the surface of protein globule in a compact manner, and the protein globule strongly affects the structure of the attached polymer, (d) that there is a strong interaction of conjugate with solvent molecules.

The revealed ability of the conjugate to undergo reversible pH-dependent phase transition from soluble to insoluble or colloid state depending on the nature of the polymer component is intriguing for understanding of protein behavior in living cell as well as for the development of new bioseparation and bioanalytical methods.

REFERENCES

1. S.V.Kazakov, N.I.Chernova, In Light scattering and photon correlation spectroscopy, Pike E.R., Abbis J.B., Eds. (Kluwer Academic Publ., The Netherland, 1997), pp. 401-422.
2. Dynamic Light Scattering, Brown W., Ed. (Clarendon, Oxford, 1993).
3. Laser Light Scattering in Biochemistry, Harding S.E., Sattelle D.B., Bloomfield V.A., Eds. (Royal Society of Chemistry, London, 1990).
4. W. Burchard, *Advances in Polymer Science* **143**:113 (1999).
5. M.B. Dainiak, V.A. Izumrudov, V.I. Muronetz et al. *Biochim. Biophys. Acta* **1381**:279 (1998).
6. V.I. Muronetz, S.V. Kazakov, M.B. Dainiak et al. *Biochim. Biophys. Acta*, in press, (2000).
7. H. Morawetz, *Macromolecules in solution*. (Wiley, New York, 1965), p. 363.
8. J. Xia, P. Dubin, In *Macromolecular complexes in Chemistry and Biology*, Dubin P., Bock J., Davis R., Schulz D.N., Thies C., Eds. (Springer-Verlag, Berlin, 1994).
9. K.V. Fokina, M.B. Dainyak, N.K. Nagradova, V.I. Muronetz, *Arch. Biochem. Biophys* **345**:185 (1997).
10. E.V. Anufrieva, T.M. Birshtein, T.N. Nekrasova, O.B. Ptitsyn, T.V. Sheveleva, *J. Polym. Sci., Part C* **16**:3519 (1968).
11. S.V. Kazakov, V.I. Muronetz, Ma.B. Dainiak, V.A. Izumrudov, I.Yu. Galaev, and B.Mattiasson, *Macromolecules* (2000), in preparation.
12. Ch. Wu and X. Wang, *Phys. Rev. Lett.* 80:4092 (1998).

Table 1. The six quantities that are obtained from the static and dynamic Zimm plots

	Static	Dynamic
Formula	$Kc / R_{\Theta}(q, c) = (1 + q^2 R_g^2 / 3) / M_w + 2A_2 c + 2A_3 c^2 + \dots$	$D(q, c) = D_o (1 + Cq^2 R_g^2 + \dots) \times (1 + k_D c + \dots)$
Experimental conditions and parameters	$qR_g < 2, A_2 M_w c < 0.5$	
	K is the optical constant, c is the concentration, R_{Θ} is the Rayleigh ratio, $q = (4\pi n_0 / \lambda_0) \sin(\Theta/2)$ is the magnitude of the scattering vector, n_0 is the refractive index of the solvent, λ_0 is the wavelength of the primary beam in vacuum, Θ is the scattering angle, η is the viscosity of the solvent, T is the absolute temperature, k_b is the Boltzmann's constant.	
Extracted molecular parameters	Weight-average molecular weight M_w (intercept) Z-average radius of gyration $R_g^2 \equiv \langle S^2 \rangle_z$ (slope at $c = 0$) The second virial coefficient A_2 (slope at $q = 0$)	Diffusion coefficient $D_o = kT / 6\pi\eta R_h$ (intercept) Architecture parameter CR_g^2 (slope at $c = 0$) k_D (slope at $q = 0$)
Equivalent sphere radii	R_g , radius of gyration is solely geometrically defined $R_T = (3A_2 M_w / 16\pi N_A)^{1/3}$, thermodynamically effective equivalent radius is defined by domains of interaction between two macromolecules	$\langle d_h \rangle = k_b T / 3\pi\eta D$, hydrodynamic diameter results from the interaction of macromolecules with the solvent

Table 2. Zimm plot data for PNIPAM/Water solutions at different temperatures

Temperature, °C	$M_w \times 10^6$, g/mol	R_g , nm	$A_2 \times 10^3$, mol ml/g ²	R_T , nm	Structure
23	2.04	100	1.11	28	Random coil
37	126	50	1.33×10^{-3}	11.8	Aggregate of Globules

FIGURE LEGENDS

Fig.1. Precipitation curve for aqueous solution of PNIPAM measured by LS

Fig.2. Typical Zimm plot for the aqueous solution of PNIPAM at 23 °C

Fig.3. pH-dependencies of radius of gyration (a) , scattering intensity (b) for the solutions of free poly(methacrylic acid) (PMAA), poly(acrylic acid) (PAA), free antibodies (Ab), and Ab-PMAA and Ab-PAA conjugates. The solid arrow indicates the position of determined isoelectric point for antibodies of 6C5 clone. The dotted arrow indicates that calculations of the radius of gyration at $\text{pH} > 4$ have not been fulfilled for the solution of Ab-PAA conjugates.

Fig.4. pH-dependencies of z-average hydrodynamic diameter (a), and polydispersity index (b) for the solutions of free poly(methacrylic acid) (PMAA), poly(acrylic acid) (PAA), free antibodies (Ab), and Ab-PMAA and Ab-PAA conjugates. The solid arrow indicates the position of determined isoelectric point for antibodies of 6C5 clone.

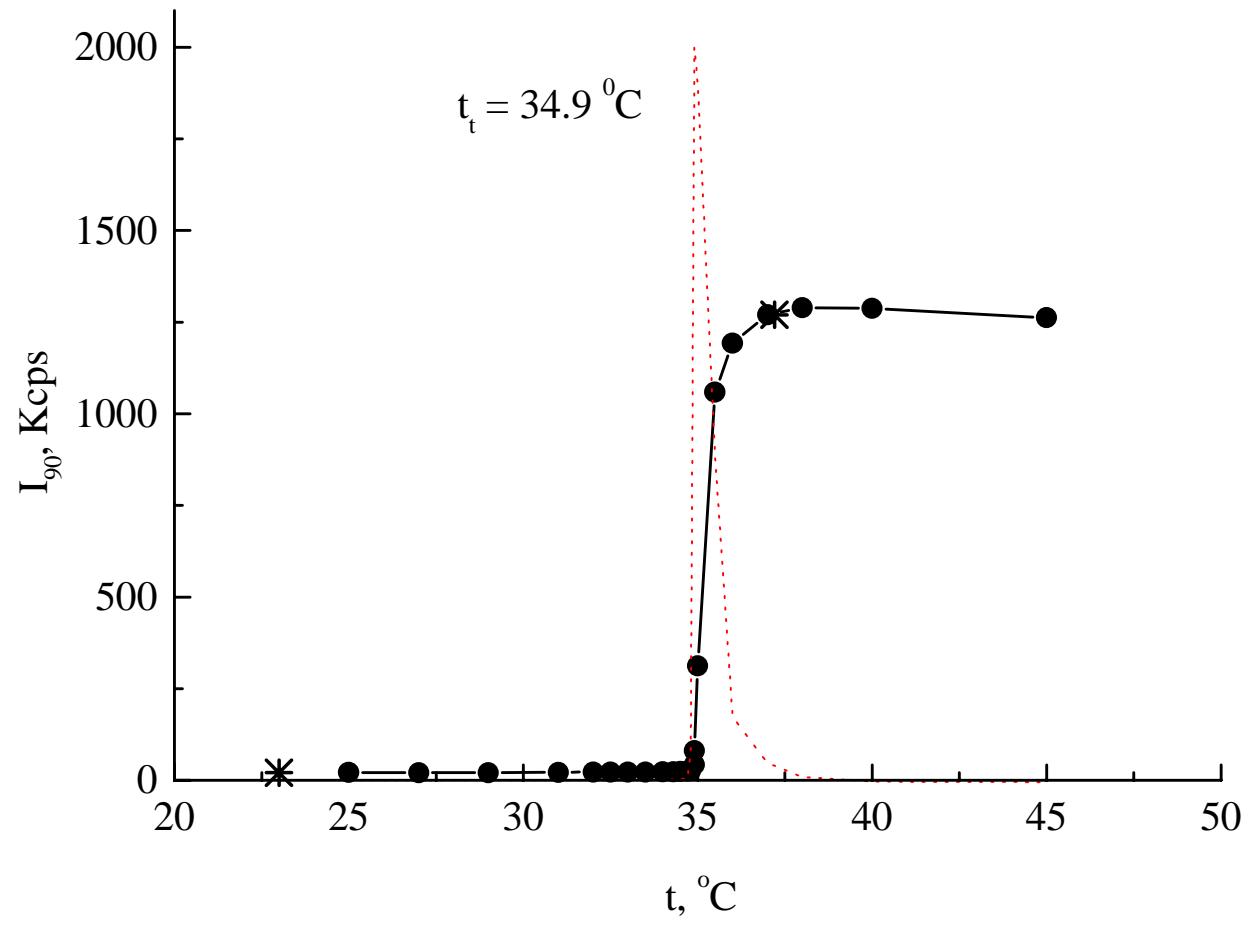


Fig.1. Kazakov, Galaev, Mattiasson

$Kc/R_{\Theta} 10^7 \text{ mol/g}$

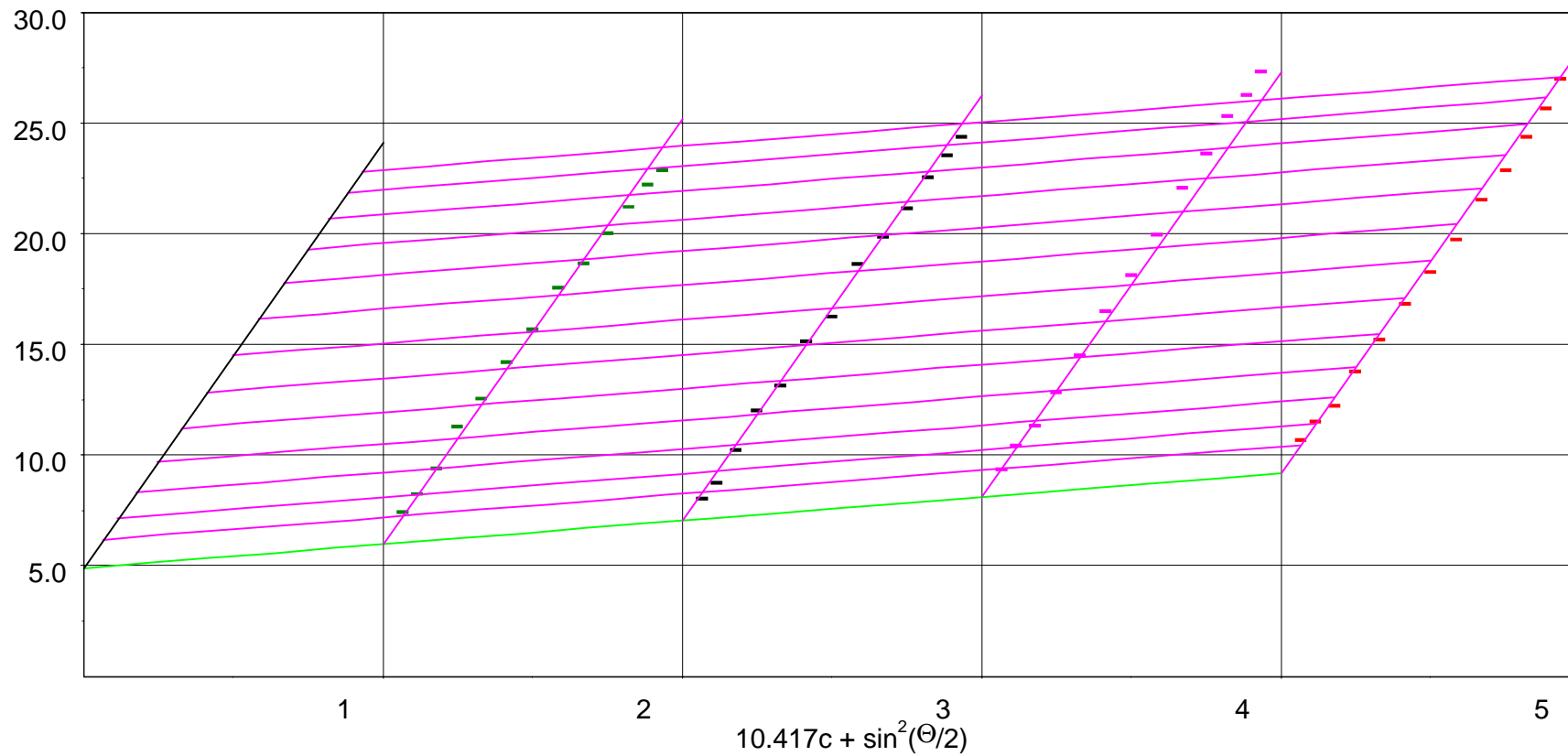


Fig.2. Kazakov, Galaev, Mattiasson

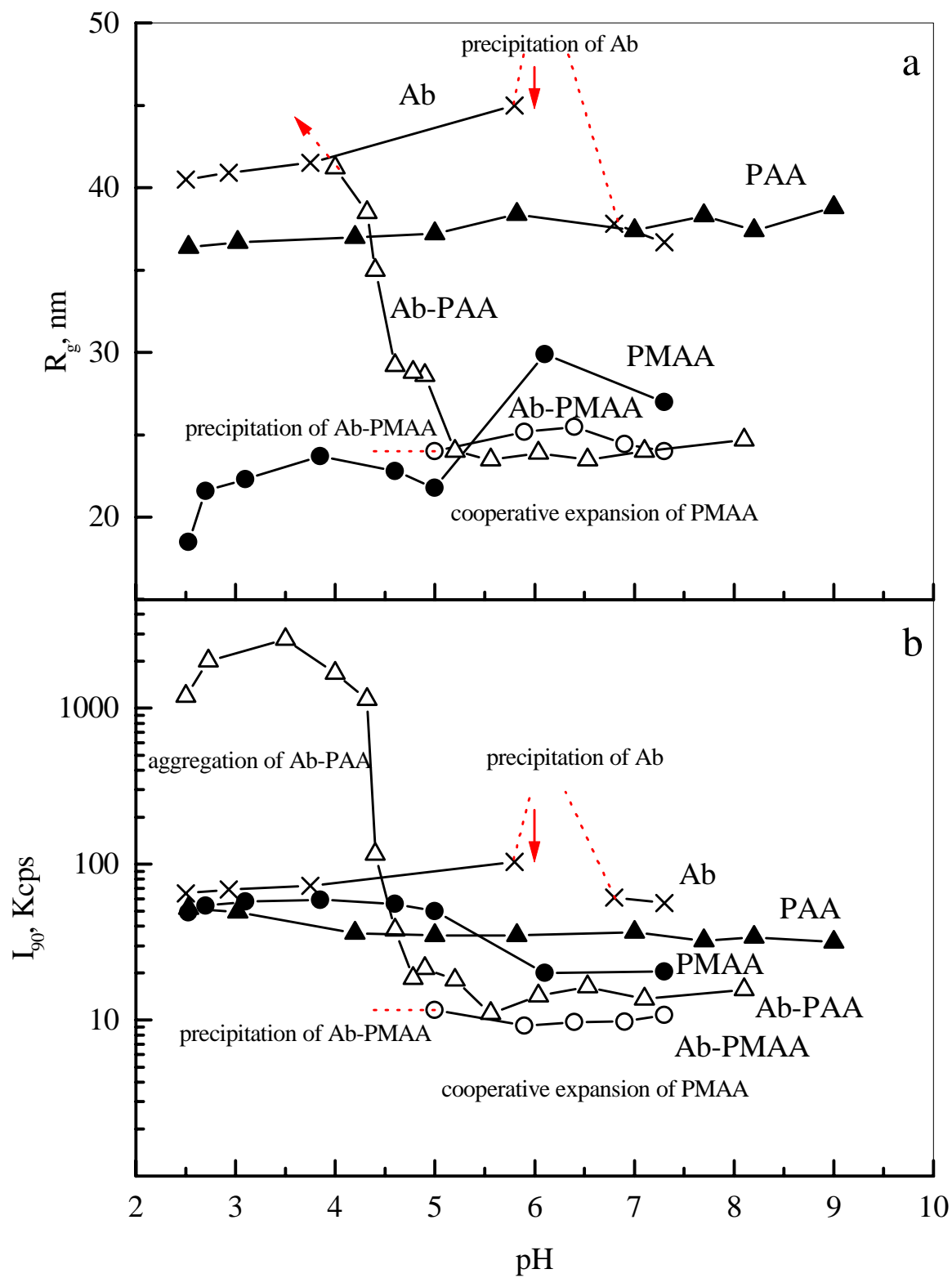


Fig.3. Kazakov, Galaev, Mattiasson

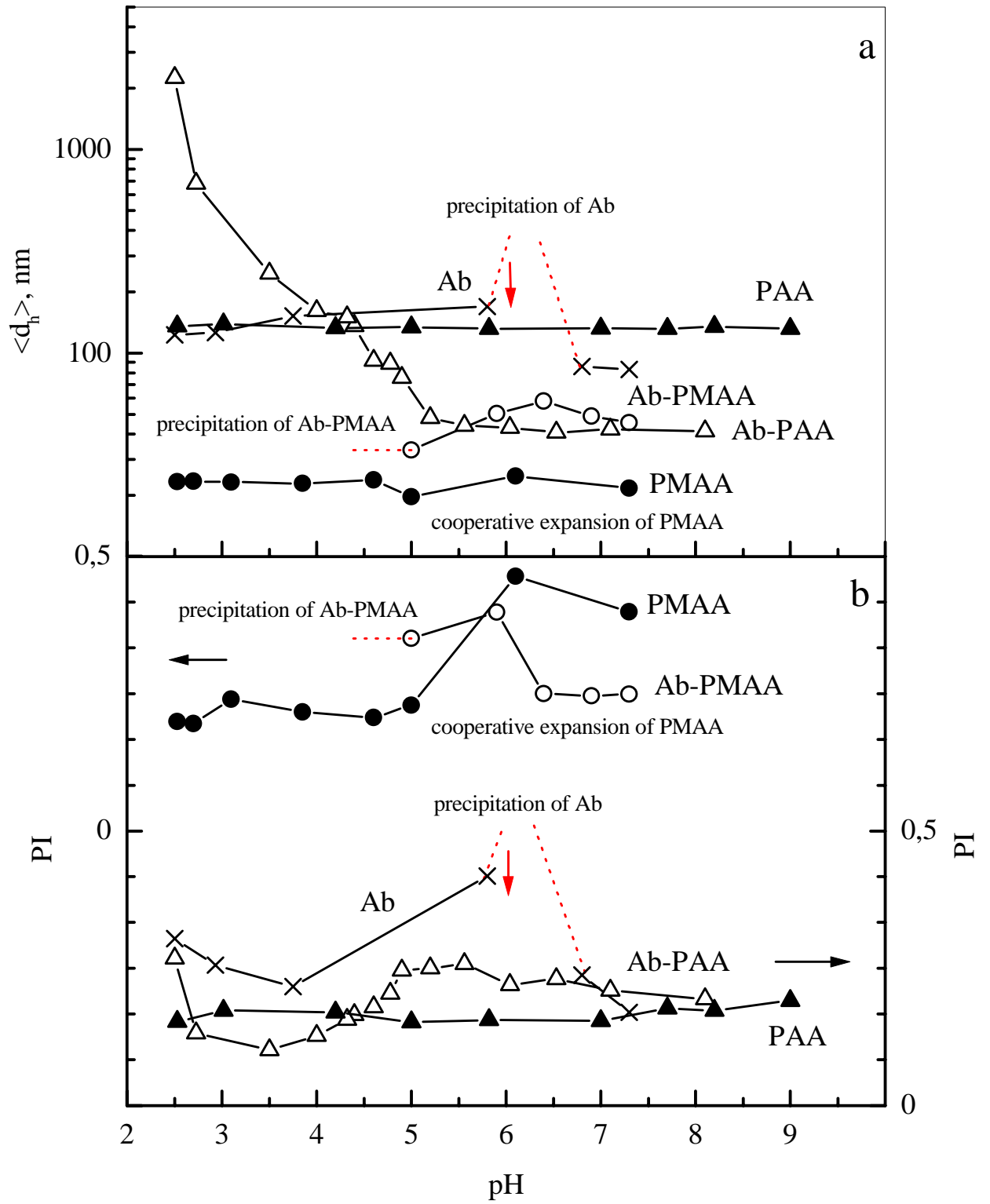


Fig.4. Kazakov, Galaev, Mattiasson